Accumulation of Neurocan, a Brain Chondroitin Sulfate Proteoglycan, in Association with the Retinal Vasculature in RCS Rats

Yiqin Zhang,[1] *Uwe Rauch,*[2] *and Maria-Thereza R. Perez*[1]

Purpose. To examine whether and how the retinal distribution of the chondroitin sulfate proteoglycan neurocan is affected after photoreceptor cell loss and whether it correlates with the multiple secondary cellular changes that accompany the photoreceptor degeneration.

Methods. Retinas from normal rats (Sprague-Dawley; postnatal days [P]0–P70), RCS rats with dystrophic retinas (P0–P300), RCS-*rdy*$^{+}$ congenic rats with nondystrophic retinas (P0–202), and rhodopsin mutant rats, P23H (P0–P257) and S334ter (P0–P220), were processed for immunohistochemistry using a polyclonal antibody to rat neurocan.

Results. The overall distribution of neurocan was similar in all retinas examined. Neurocan immunostaining was detected over the nerve fiber layer, the plexiform layers, the photoreceptor outer segments region, and the ciliary epithelium. With age, labeling throughout the plexiform layers decreased continuously. In RCS rats however, conspicuous labeling was also seen in association with retinal vessels, from P15 onward.

Conclusions. Accumulation of neurocan in association with the retinal vasculature does not correlate with photoreceptor cell loss, because it was not observed in the rhodopsin mutant rats. During the earliest stages of the disease, accumulation of debris in the subretinal space in RCS rats may be sufficient per se to initiate a cascade of metabolic changes that result in accumulation of neurocan. With time, the neurocan accumulated perivascularly may, by interaction with other matrix molecules, modulate at least some of the vascular alterations observed in this animal model. (*Invest Ophthalmol Vis Sci.* 2003; 44:1252–1261) DOI:10.1167/iovs.02-0450

Chondroitin sulfate proteoglycans (CS-PGs) constitute a subclass of proteoglycans consisting of a core protein to which one or more sulfated glycosaminoglycan side chains are covalently attached (see, e.g., Ref. 1). Different core proteins and variations in the size, structure, and degree of sulfation of the glycosaminoglycan chains account for the diversity in CS-PGs that have thus far been identified. These macromolecules are found mostly in cartilage and in the central nervous system as components of the extracellular matrix and also in association with cell membranes.[1] Whereas in cartilage, aggregates of highly hydrated proteoglycans are primarily responsible for the physical properties of this tissue, their function in the central nervous system is elusive. In the latter, CS-PGs are mainly expressed during development and in response to injury, both situations characterized by high plasticity of the tissue.[2]

In the retina, biochemical and cytochemical methods also reveal the presence of structurally distinct CS-PGs and it appears that photoreceptor cells, inner retinal neurons, retinal glial cells, and the retinal pigment epithelium (RPE) are capable of synthesizing these molecules. Accordingly, CS-PGs have been localized in the interphotoreceptor matrix, in the synaptic layers, in the nerve fiber layer, and at the level of the inner limiting membrane.[3–14]

As in other tissues, retinal proteoglycans seem to play a role, not only in the development and functioning of the normal retina, but also in pathologic processes. Alterations of the structure and chemical composition of the interphotoreceptor matrix have been observed in animal models of retinitis pigmentosa (RP), and occur both when the defect lies in the photoreceptors themselves and when the RPE is defective. Most changes are likely to occur secondary to photoreceptor cell degeneration, but have in some instances also preceded the degeneration, suggesting that alterations in the distribution of proteoglycans may in part contribute to the cell loss.[15–18] Proteoglycan levels are also likely to play a role in the secondary pathology that is observed in the retinas of animal models and of patients with RP. A number of cellular changes are noted after photoreceptor cell degeneration, such as loss of other neuronal cells, activation of glial cells, sprouting of neurites, and vascular degeneration and proliferation.[19–22] All these changes involve dynamic cell–cell and cell–matrix interactions and are therefore also likely to be preceded and/or accompanied by alterations in the levels of proteoglycans and of their receptors/ligands.

The purpose of the present study was to examine the distribution of the CS-PG neurocan in dystrophic rat retinas. Neurocan, a member of the lectican family of hyaluronan-binding proteoglycans is one of the most abundant PGs in developing brain tissue, and its structure and interactions point to a role in the organization of the matrix and in the modulation of normal developmental processes.[23–25] Neurocan has been detected in the innermost retinal layers in embryonic rat retinas and in the plexiform layers during the first postnatal weeks.[3,13,26,27] However, reexpression of neurocan has been reported in adult rats after transient retinal ischemia,[28] conforming with other reports showing that the expression of this CS-PG is upregulated after nerve tissue injury.[29–31]

Using immunocytochemistry, we thus examined the distribution of neurocan in retinas of Royal College of Surgeons (RCS) rats and of P23H and S334ter transgenic rats. In RCS rats, a mutation in the gene encoding the receptor tyrosine kinase

From the [1]Wallenberg Retina Center, Department of Ophthalmology, and the [2]Department of Experimental Pathology, Lund University, Lund, Sweden.

Supported by the Faculty of Medicine of the University of Lund; Grant 12209 from the Swedish Medical Research Council (MTRP); Grant B650-19981127/2001 from the Swedish Natural Sciences Research Council (UR); the Crown Princess Margareta's Committee for the Blind; the Swedish Society for Medical Research; the K. A. Wallenberg, Crafoord, A. Österlund, C. Groschinsky, T. E. Segerfalk, and Syskonen Svensson Foundations; and the Foundation Fighting Blindness.

Submitted for publication May 6, 2002; revised August 27, 2002; accepted September 20, 2002.

Commercial relationships policy: N.

The publication costs of this article were defrayed in part by page charge payment. This article must therefore be marked "*advertisement*" in accordance with 18 U.S.C. §1734 solely to indicate this fact.

Corresponding author: Maria-Thereza R. Perez, Wallenberg Retina Center, Department of Ophthalmology, Lund University, Klinikgatan 26, BMC, B13, S-221 84, Lund, Sweden; maria_thereza.perez@oft.lu.se.

MERTK,[32] results in defective phagocytosis of shed rod outer segment disc membranes by the RPE, ultimately leading to photoreceptor cell degeneration.[33,34] As the disease progresses, the entire retina is affected and ganglion cell loss, activation of glial cells, neovascularization of the RPE, and formation of vitreoretinal membranes are also observed.[21,35–38] In P23H and S334ter rats, degeneration results from rhodopsin mutations and, as such, is a primary photoreceptor event,[39,40] as opposed to the situation in RCS rats. Vascular changes have been previously observed in other models of retinal degeneration, including a P23H transgenic mouse,[41–43] and alterations in proteoglycan levels can therefore be expected.

Materials and Methods

Experimental Animals

The experiments were conducted with the approval of the local animal experimentation ethics committee. Animals were handled according to the guidelines on care and use of experimental animals set by the Government Committee on Animal Experimentation at the University of Lund and the ARVO Statement for the Use of Animals in Ophthalmic and Vision Research. The animals examined included Sprague-Dawley rats, postnatal days (P)0 to P70, (n = 30), RCS-*rdy*$^+$ rats with nondystrophic retinas (P0–P202, n = 12), RCS rats with dystrophic retinas (pink-eyed, tan-hooded, P0–P300, n = 59), P23H rats (line 1; P0–P257, n = 35), and S334ter rats (line 4; P0–P220, n = 24). Homozygous breeders of P23H and S334ter rats were produced by Chrysalis DNX Transgenic Sciences (Princeton, NJ), and developed and provided by Mathew M. LaVail (University of California, San Francisco, CA). Analysis was performed on heterozygous animals obtained by mating with wild-type Sprague-Dawley rats. All animals were maintained on a 12-hour light–dark cycle. The younger animals were killed by decapitation, and older animals were anesthetized with carbon dioxide before decapitation.

Tissue Preparation

Eyes were quickly enucleated and immersed in a freshly prepared solution of 4% formaldehyde in Sörensen buffer (0.1 mM; pH 7.2). Small eyes were kept in fixative for 2 hours. In larger eyes, the anterior segment, lens, and vitreous bodies were removed 10 minutes after immersion in fixative. The posterior segments were transferred to fresh fixation medium (as just described) and kept at 4°C for two additional hours. The tissue was subsequently rinsed and cryoprotected in Sörensen buffer containing sucrose. The tissue was embedded in an albumin-glycerin medium (30 g egg albumin, 3 g gelatin, 100 mL distilled water) and frozen. Sections were obtained on a cryostat (12 μm), collected on gelatin-chrome alum–coated slides, air dried, and stored at −20°C until used. A few of the sections processed for neurocan immunoreactivity were photographed and subsequently counterstained with hematoxylin and eosin. After fixation and cryoprotection, some retinas were instead dissected from the RPE and mounted with the vitreous side up on glass slides.

Antibodies

Antibodies included neurocan, a polyclonal antiserum, raised in rabbits immunized with immunoaffinity-purified rat neurocan and boosted with recombinant rat neurocan produced in mammalian cells[44,45]; RECA, a mouse anti-rat RECA-1 antigen, which recognizes a cell surface antigen distributed on all vascular endothelium (Serotec, Oxford, UK); and cytokeratin, a monoclonal mouse anti-human cytokeratin (MNF-116; Dako, Glostrup, Denmark).

Immunocytochemistry

Cryostat sections and wholemounted retinas were incubated for 90 minutes with 0.1 mM PBS containing 1% BSA, 0.25% Triton X-100 (PBTx), and 5% normal serum, followed by overnight incubation at 4°C with rabbit anti-neurocan serum (1:1000 in PBTx containing normal serum). For colocalization studies, primary antibodies were applied in combination (neurocan, 1:1000; RECA-1, 1:100; cytokeratin, 1:40). After they were rinsed, sections were incubated for 90 minutes with Texas red sulfonyl chloride-conjugated donkey anti-rabbit (1:100; Jackson ImmunoResearch, West Grove, PA) and/or fluorescein isothiocyanate–conjugated goat anti-mouse. After they were immunostained, sections were rinsed and mounted with buffered glycerol containing the antifade agent phenylenediamine (Merck, Darmstadt, Germany). To verify the specificity of the neurocan labeling, the diluted neurocan antiserum was preincubated with affinity-purified neurocan for 24 hours before application to the sections, and the neurocan antiserum was excluded from the incubation. Sections were viewed with a light microscope equipped for fluorescence microscopy, and micrographs were taken with a digital camera. The images were processed with Photoshop (Adobe, San Jose, CA).

Western Blot Analysis

Frozen (−80°C) pieces of retinal or brain tissue of 8-day-old (P8) or adult rats (P60) were homogenized in TBS buffer containing protease inhibitors. After adjustment of the protein concentrations, extracts were partially treated with chondroitinase avidin-biotin complex (ABC). The extracted proteins were separated by 5% SDS-PAGE and transferred to polyvinylidene difluoride (PVDF) membranes (Hybond-P; Amersham, Uppsala, Sweden). The membranes were incubated with the polyclonal antibody against neurocan and developed with horseradish peroxidase–conjugated secondary antibody, with an enhanced chemiluminescence detection system ((ECL+; Amersham).

Results

Immunocytochemistry

Between P0 (day of birth) and P12, differences in the accumulation of neurocan were observed between the central and peripheral retinas, reflecting a center-to-periphery gradient that appeared to parallel the center-to-periphery maturation of the retina. The same observation was made in normal (illustrated in Figs. 1D–F), RCS, and in transgenic rats. To facilitate comparison, however, the distribution observed in the midperiphery will be given in the subsequent descriptions, unless stated otherwise.

Normal Rats: Sprague-Dawley and RCS Rats with Nondystrophic Retinas

At the ages examined, no differences were noted between the distribution of neurocan in Sprague-Dawley rats and in RCS rats with nondystrophic retinas. Both will therefore be referred to as normal retinas (control subjects) in the present study.

Figure 1 illustrates the distribution of neurocan immunoreactivity in normal retinas. At P0, intense labeling was observed in the posterior part of the optic nerve (Fig. 1A), in the inner retina (Fig. 1B), and in the ciliary epithelium (Fig. 1C). In the retina, intense and diffuse neurocan immunoreactivity was found in the developing inner plexiform layer (IPL; Fig. 1B), and it was possible to discern a number of immunonegative cell profiles within this layer. Labeling was also noted in radial strands in the proximal neuroblastic layer, next to the IPL. No major differences were noted at P3, except that a discrete sublayering was observed in the IPL and more diffuse labeling was seen in the inner two thirds of the neuroblastic layer (Figs. 1D, 1E). At P5, a localized labeling was observed within the developing inner nuclear layer (INL; Fig. 1G). Figure 1H shows the same section as in 1G, which was counterstained after being immunoprocessed and photographed. The accumulation of neurocan labeling occurred in a region where no cell bodies were noted, delineating a more proximal region within the INL

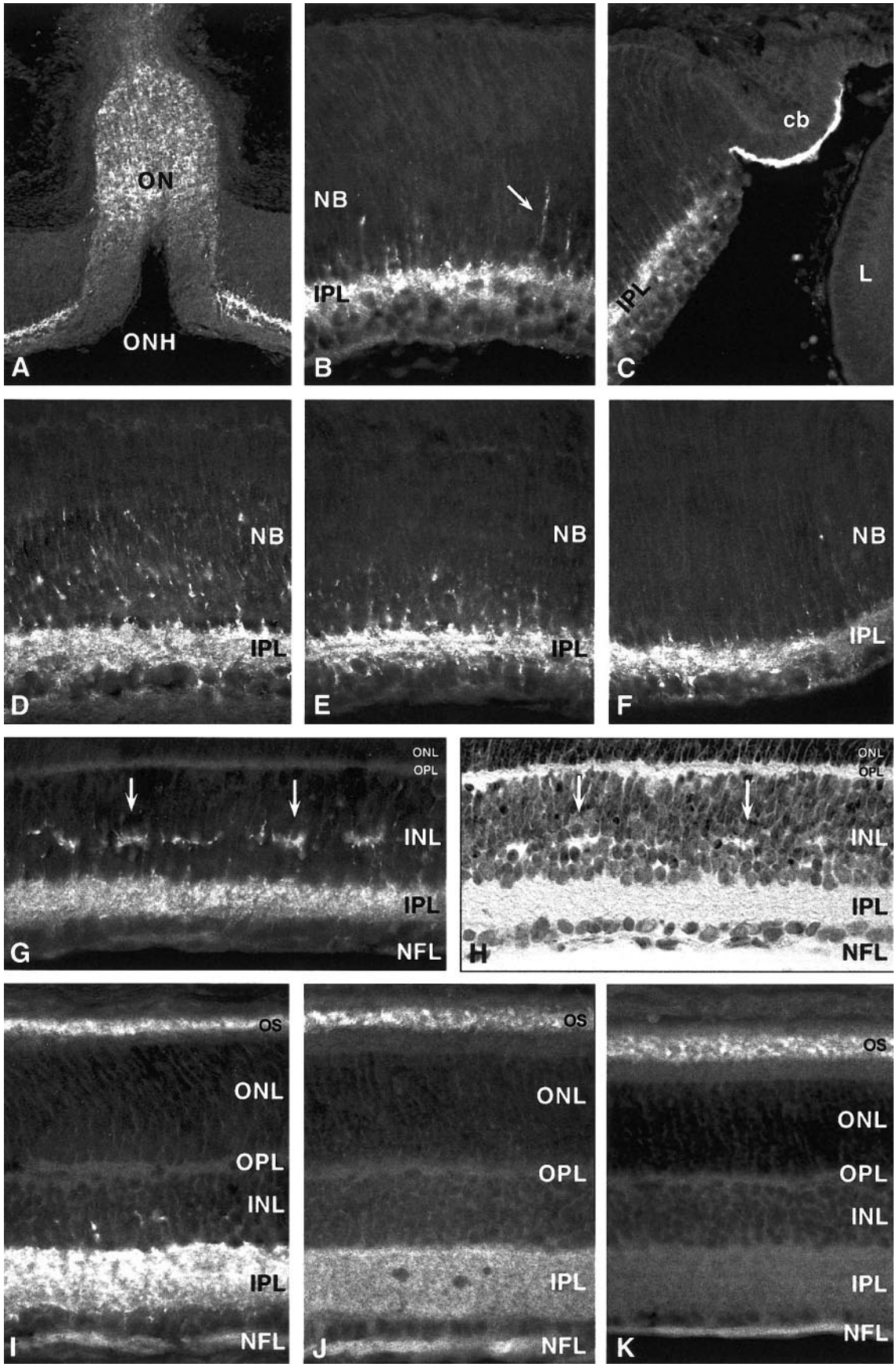

that exhibited rounder cell bodies, and a distal region where the cell bodies were more tightly packed and where most still exhibited an oval shape (Fig 1H). At this time point, weak labeling was also seen in the nerve fiber layer (NFL; Fig. 1G) and as a thin line in the subretinal space (not shown).

By P12, staining in the retina was almost completely restricted to the IPL, the NFL, and the region corresponding to the photoreceptor outer segments (Fig. 1I). Between P12 and P70, no significant differences in the distribution of immunolabeling were noted, but whereas immunoreactivity throughout the ciliary epithelium, the posterior region of the optic nerve, the photoreceptor outer segments, and the NFL remained intense, labeling in the IPL gradually decreased with age (Figs. 1J, 1K).

Neurocan staining was also observed on rare occasions in association with a large superficial retinal vessel (not shown).

RCS Rats

Between P0 and P12, the distribution of neurocan immunoreactivity resembled that observed in control retinas, both when compared with RCS nondystrophic retinas and with retinas of Sprague-Dawley rats. This distribution is illustrated in Figures 2A and 2B, which show neurocan in the midperiphery of RCS rat retinas at P0 and P12, respectively. Labeling throughout the plexiform layers, the NFL, and the ciliary epithelium was also comparable to that of normal retinas at all ages examined.

At P15, however, distinct labeling was observed in association with several large superficial blood vessels at the level of the optic nerve head (Fig. 2C). With increasing age, this type of labeling was seen in all retinal eccentricities (Fig. 2H). Staining was also present at P35 and onward, coinciding with vascular profiles at the level of the outer plexiform layer (OPL), with vessels running between the vitreous retinal surface and the OPL, and vessels running along with the nerve fiber bundles (Figs. 2D–I). Figure 2E depicts the same section as Figure 2D, which was counterstained after being immunoprocessed and photographed, and shows that the accumulation of neurocan labeling across the IPL and INL coincided with a vascular profile. In older animals, immunoreactivity was also detected in association with retinal blood vessels reaching the RPE (described later).

Increased neurocan labeling also appeared in areas associated with the debris zone in the subretinal space at all ages examined (Figs. 2F–H).

Colocalization of Neurocan with RECA and Cytokeratin in RCS Retinas

Neurocan and RECA. Retinal tissue obtained from RCS rats with dystrophic retinas (sections and wholemounted retinas) were processed for simultaneous localization of neurocan and rat endothelial cell antigen (RECA). Figures 3A–D show neurocan immunoreactivity associated both with larger RECA-labeled superficial vessels (Fig. 3A) and smaller intraretinal vessels (Figs. 3B–D). It was not possible to establish the exact site of accumulation, but neurocan immunoreactivity appeared to be concentrated around the vessels (Figs. 3A–D).

Neurocan and Cytokeratin. Staining of epithelial cells with anti-cytokeratin resulted in labeling in the position of the RPE at all ages examined. By P75 and onward, cytokeratin labeling was also present at various levels within the retina, and in some sections, cytokeratin and neurocan immunoreactivities were associated with the same vascular profiles (Figs. 3E, 3F).

P23H and S334ter Rats

The overall distribution of neurocan immunostaining in P23H and S334ter rat retinas appeared similar to that seen in control retinas, except for labeling throughout the photoreceptor outer segments, which disappeared as photoreceptor cells were lost. Increased accumulation of neurocan was occasionally noted in older animals at the level of the NFL in association with larger superficial vessels (Fig. 4). However, the incidence of this type of labeling did not seem to be higher than in control retinas. Further, abnormal accumulation of neurocan in association with intraretinal vessels was not observed in these specimens at any of the time points examined: P23H rats (P0–P257), S334ter rats (P0–P220).

Antibody Specificity

In sections incubated with secondary antibodies alone, weak signal was detected throughout the photoreceptor inner and outer segments in normal animals and in the debris zone in the RCS dystrophic rat retinas (not shown). After incubation of sections with the preadsorbed neurocan antiserum, no specific immunolabeling was detected in the ciliary epithelium, the optic nerve, or the retina of normal rats (Figs. 5A, 5B) or of rats with dystrophic retinas (Figs. 5C, 5D and 5E, 5F). In Western blot analysis, no cross-reactivity of the neurocan antiserum with brevican, one of the most closely related molecules, was observed.[44] No staining was detected in brain extracts from neurocan-knockout mice, further confirming the specificity of the antiserum.[45]

Western Blot Analysis

Normal Rats: Sprague-Dawley and RCS Rats with Nondystrophic Retinas. In 8-day-old rat brain tissue, proteolytically unprocessed neurocan molecules are the predominating form. Chondroitinase ABC treatment converts these molecules (due to the heterogeneous glycosaminoglycan substitution, appearing as a smear well above 250 kDa) to a homogenous core protein appearing with a stronger signal as a well-defined band of 250 kDa. At 150 kDa, the much less abundant core protein of the C-terminal proteolytic fragment is also apparent, whereas the more heterogeneous signal of this fragment in its glycosaminoglycan-substituted form was too dilute to be detected. Similar to brain tissue, after elimination of the glycosaminoglycan modification by chondroitinase ABC, a core protein of 250 kDa corresponding to the unprocessed neurocan molecule was clearly observed in the retina at P8. A weak band of 150 kDa corresponding to the core protein of the C-terminal processing product was also detected (Fig. 5G). At P60, only a very weak core protein band of 150 kDa was noted.

FIGURE 1. Neurocan immunoreactivity in normal retinas at P0 to P70. (**A–C**) At P0, labeling was observed (**A**) in the posterior part of the optic nerve (ON) and in the inner retina at the level of the optic nerve head (ONH) region; (**B**) in the IPL and in radial strands (*arrow*) in the proximal neuroblastic layer (NB) in the midperiphery; and (**C**) in the IPL and the ciliary epithelium in the periphery. (**D–F**) Neurocan distribution at P3 illustrating a center-to-periphery gradient, in which more extensive labeling is seen throughout the neuroblastic layer (NB) in the central retina (**D**) than in the midperiphery (**E**), or in the periphery (**F**). At P5—(**G**) neurocan immunolabeling, (**H**) hematoxylin-eosin staining of the same section—labeling was present in the IPL, weakly in the OPL and the NFL, and in the INL. In the latter, accumulation (*arrows*) seemed to coincide with a region that delineated two areas within the INL: a more-developed proximal area and a less-developed distal area. At P12 (**I**), P25 (**J**), and P70 (**K**), intense labeling was present over photoreceptor outer segments (OS) and the NFL, whereas in the IPL staining intensity decreased with age. ON, optic nerve; ONH, optic nerve head; NB, neuroblastic layer; cb, ciliary body; L, lens.

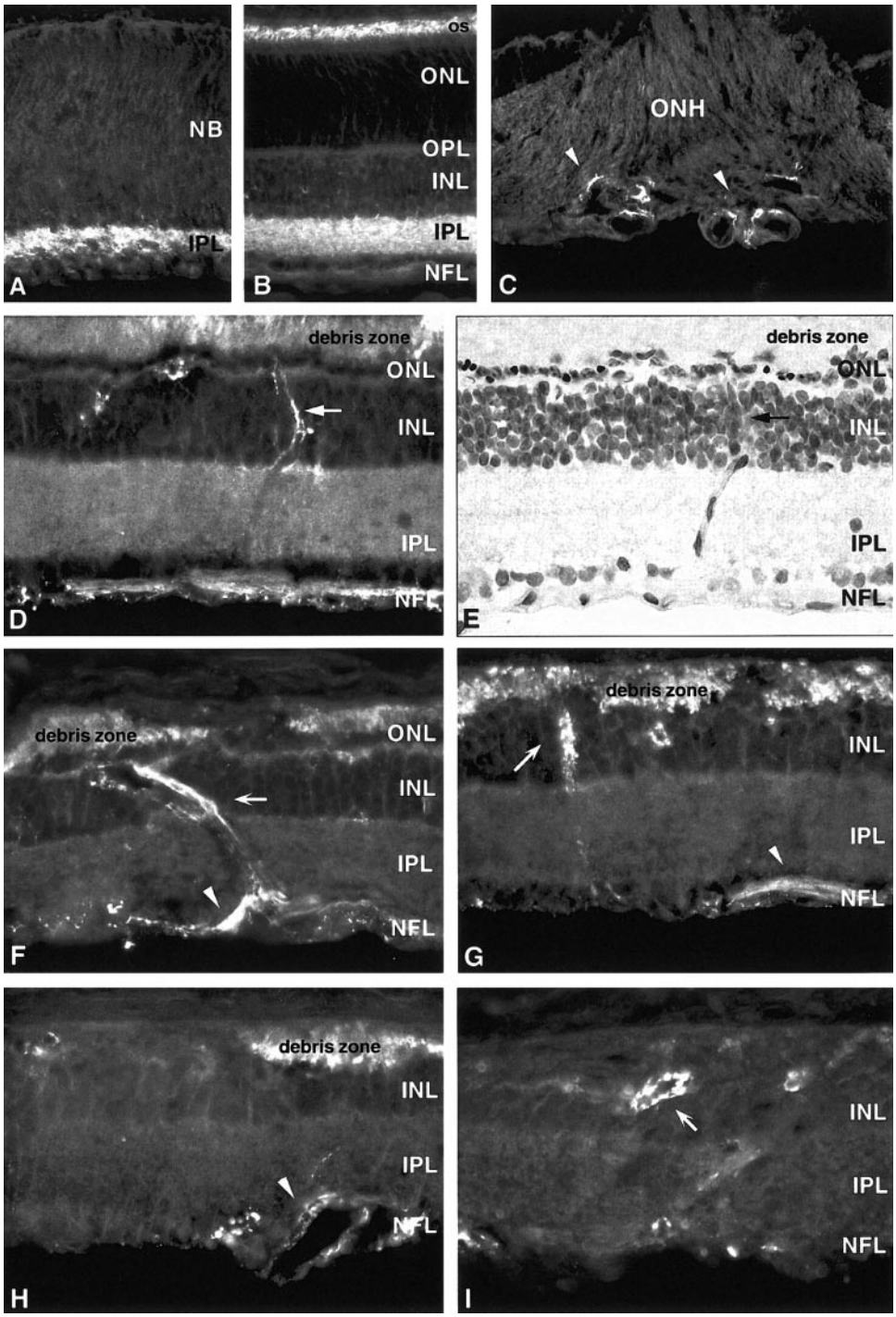

FIGURE 2. Neurocan immunoreactivity in RCS rat retinas at P0 to P300. In the midperiphery of P0 retinas (**A**), labeling appeared as in normal retinas in the IPL. At P12 (**B**), the distribution of labeling still corresponded to that of normal retinas, with intense labeling of photoreceptor outer segments (OS), IPL, and NFL. At P15 (**C**), labeling accumulated surrounding large vessels (*arrowheads*) at the level of the optic nerve head (ONH). From P35 onward, labeling also accumulated in association with vessels traversing the retina (**D–I**, *arrows*), in the nerve fiber layer (**F–H**, *arrowheads*), and in the debris zone in the subretinal space (**D–H**): at P39—(**D**) neurocan immunolabeling, (**E**) hematoxylin-eosin staining of the same section—(**F**) P70, (**G**) P140, (**H**) P180, and (**I**) P300. Designation of layers as in Figure 1 and the text.

RCS Rats. At P8, no differences were noted compared with normal retinas. At P60, however, a weak band of 250 kDa and a strong band of 150 kDa were observed (Fig. 5G). This latter form was even evident without chondroitinase ABC treatment, appearing as a smear between 150 and 250 kDa, which disappeared after the treatment.

DISCUSSION

Normal Rats

A strong band of 250 kDa, likely to be equivalent to the 220-kDa band observed by Inatani et al.,[13] and a weaker band of 150 kDa were seen after chondroitinase ABC treatment of P8 retinal homogenates, in contrast to their report, in which the 150-kDa band became the dominant form at this early age. However, the monoclonal antibody that they used is likely to detect only one epitope in both neurocan forms, whereas the antiserum used in the present study also detects epitopes in N-terminal regions not present in the 150-kDa form.

The distribution of neurocan during postnatal rat retinal development in our study otherwise agrees to a great extent with the observations made by Inatani et al.[13] Transient expression was observed in the retina in areas of fiber outgrowth, which supports the notion that neurocan plays a role also in

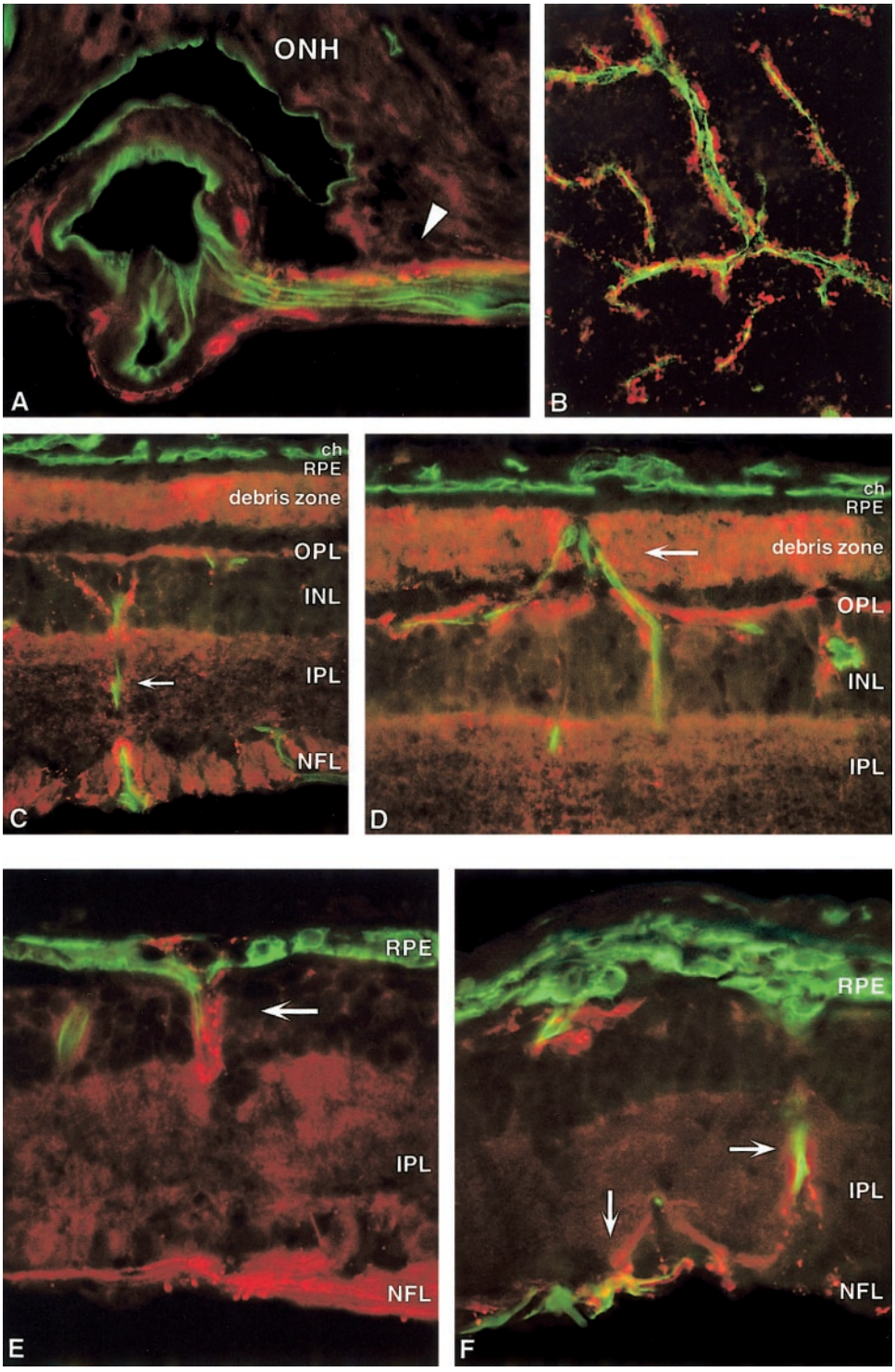

FIGURE 3. (**A**–**D**) Dual labeling of RCS rat retinal sections for neurocan (*red*) and RECA (*green*) immunoreactivities. (**A**) Neurocan labeling (*arrowhead*) in association with a large vessel at the level of the optic nerve head (ONH) region at P25. (**B**) Neurocan and RECA immunoreactivities in a wholemount preparation of a P40 RCS rat retina. (**C**, **D**) Neurocan labeling in retinas from P35 and P45, respectively, in association with vessels traversing the retina (*arrows*), some reaching the RPE. (**E**, **F**) Dual labeling of RCS rat retinal sections for neurocan (*red*) and cytokeratin (*green*) immunoreactivities. (**E**) Corresponds to a P112 RCS rat retina where cytokeratin labeling was observed within the retina and in association with neurocan staining (*arrow*). (**F**) Cytokeratin labeling within the retina and in the vitreous surface of the retina in a P135 RCS rat retina, again coinciding with accumulation of neurocan (*arrows*). ch, choroid.

the retina in directing dendritic and axonal outgrowth.[46,47] Immunoreactivity was seen also pericellularly in the developing neuroblastic layer and in the ganglion cell layer. At P5, accumulation of labeling was observed in patches within the INL that appeared to delineate two levels of differentiation within this layer. In addition, a number of immunolabeled radial profiles were observed in the developing INL that, as suggested by Inatani et al.,[13] seemed to correspond to accumulation in or in association with Müller cell processes. Such labeling was observed only during the first two postnatal weeks, suggesting that neurocan could also participate as a regulator of cell migration in the developing retina.

In adult retinas, neurocan immunolabeling was detected in the subretinal space. The same distribution has not been observed previously[13] and may be due to differences in the processing of the tissue sections. It is possible that the shorter fixation protocol used in the present study favored the detection of labeling in the outer retina. In addition, the polyclonal antiserum used in this study also detects, as mentioned earlier, the hyaluronan-binding N-terminal part of the molecule. Hya-

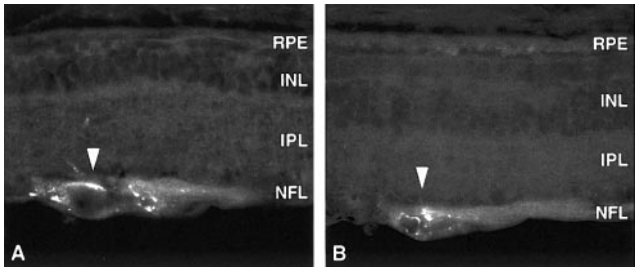

FIGURE 4. Neurocan immunoreactivity in (**A**) P23H rat retinas (P170) and (**B**) S334ter rat retinas (P96). Micrographs illustrate the accumulation of neurocan that was occasionally observed in these animals in association with superficial retinal vessels, at the level of the NFL (*arrowheads*).

luronan and proteoglycans have been shown to be among the major constituents of the interphotoreceptor matrix (IPM) in rodents and in other species and have been suggested to play a role, for instance, in adhesion of the retinal pigment epithelium.[4,5,8,48–51] Further, the matrix metalloproteinase (MMP)-2, identified as a protease likely to process neurocan,[52] is present in the IPM,[53] further suggesting that neurocan is a component of the IPM. The onset of accumulation of neurocan in the IPM in the present study coincides with the appearance of outer segments at P5,[54] suggesting that neurocan could be involved in photoreceptor outer segment development and/or maintenance.

Weak neurocan immunolabeling was also observed in adult rat retinas in the NFL. It was not possible to determine unequivocally which neurocan form is present at this time point, but MMP-2 has been shown to be constitutively expressed in retinal ganglion cells and their axons,[55] suggesting that in the retina a developmentally increasing fraction of neurocan may be proteolytically processed, as previously observed in brain tissue.[23]

The distribution of neurocan in the retina in the present study confirms previous studies showing that its expression is developmentally regulated,[25] and suggests also that neurocan may be involved in different processes in different parts of the retina. It should be noted, however, that no obvious morphologic defects have been observed in Nissl staining of brain sections[45] or in hematoxylin-eosin–stained retinal sections (Perez M-TR, unpublished observations, 2001) from neurocan-null mice, whereas deficits in synaptic plasticity were observed in the hippocampus of these animals.[45] These observations suggested some redundancy among lecticans or other proteoglycans in defining structure.[45] However, they indicate also that neurocan plays a functional role (possibly also in the retina) at least in some processes, that cannot be fully compensated for by other molecules.

RCS, P23H, and S334ter Rats

In P23H and S334ter rats, the distribution of neurocan remained comparable to that of normal retinas, despite the progressive photoreceptor cell loss. In RCS rats however, an increased accumulation of neurocan was present throughout the photoreceptor outer segments. As mentioned earlier, the IPM is rich in glycoproteins and proteoglycans, and alterations in the levels and distribution of some of these molecules have been observed in RCS rats.[15,56,57] The increased accumulation of neurocan in the subretinal space appeared to parallel the gradual build-up of undigested disc membranes, and at late stages neurocan was present even in areas where photoreceptors were lost and only a debris zone remained, suggesting that the accumulation may reflect mainly delayed degradation of neurocan rather than increased synthesis. This could explain why a similar subretinal accumulation of neurocan was not noted in P23H and S334ter rats, in which phagocytosis of shed outer segments appears to function normally.

In RCS rats, a conspicuous accumulation of neurocan was also present in association with the retinal vasculature. A similar accumulation of neurocan or of other members of the lectican family has not to our knowledge, been described previously. After a lesion of the entorhinal cortex in adult rats, for example, a strong upregulation of neurocan was observed in the fascia dentata, with no particular deposition around the basal lamina of blood vessels.[29] However, our observations seem consistent with previously reported alterations in the

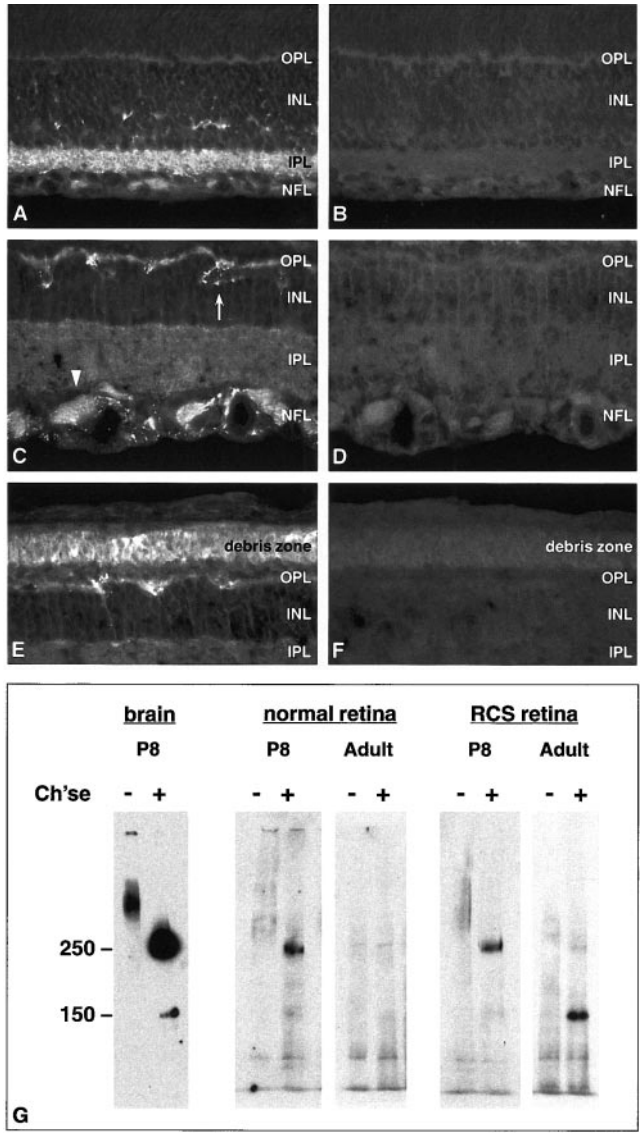

FIGURE 5. (**A**, **C**, **E**) RCS rat retinal sections incubated with neurocan antiserum. (**B**, **D**, **F**) Consecutive sections incubated with preadsorbed neurocan antiserum. The characteristic labeling—at (**A**) P5 in the NFL, IPL, INL; at (**C**) P35 in association with superficial vessels at the level of the NFL (*arrowhead*) and intraretinal vessels (*arrow*); and at (**E**) P50 in the debris zone—was not observed in the corresponding consecutive sections (**B**, **D**, **F**). (**G**) Western blot analysis of neurocan in brain and retinal tissues obtained from normal and RCS rats (P8 and P60). After chondroitinase (Ch'se) treatment of tissue extracts (+), 250- and 150-kDa bands were observed in the tissues of normal and RCS rats at P8. A strong band also appeared at 150 kDa in extracts from adult RCS rat retinas.

composition of the extracellular matrix (ECM) and in the thickness of the matrix layer surrounding the retinal vessels in RCS rats.[38,58] In these animals, the most severe vascular changes involve vascular contraction, vascularization of the RPE, vascular proliferation, and formation of vitreoretinal membranes,[33,58,59] changes that are generally thought to be secondary to photoreceptor cell death.

However, actual pathologic loss of photoreceptors is believed to begin in RCS rats at around P20,[33] and we found an accumulation of neurocan around central vessels as early as P15, suggesting that it does not occur, at least initially, as a result of the photoreceptor cell loss. On the other hand, an abnormal accumulation of disc membranous debris is noticeable in RCS rats at around P12,[33,60] and alterations in the distribution of certain IPM components are present before the period of degenerative photoreceptor cell loss.[15,61] The early accumulation of neurocan around vessels in RCS rats could thus be triggered by changes in the biochemical environment of the subretinal space as membranous discs start to accumulate. Müller cells, which span radially the entire thickness of the retina, could in this case convey signals and/or transport molecules from the subretinal space to the remainder of the retina. Degeneration of perivascular Müller cell processes has been reported in RCS rats, which, as suggested by Roque and Caldwell,[62] could result in alterations in the ECM and thereby in alterations of endothelial cell function.

An abnormal accumulation of the MMP inhibitor, tissue inhibitor of metalloproteinase (TIMP)-3 has been observed in association with the retinal vasculature in human retinas with retinitis pigmentosa.[63] Reduced proteolysis by TIMP-3 or other proteinase inhibitors could occur in RCS rat retinas, resulting in accumulation of various components of the perivascular matrix, including neurocan. With time, the accumulated neurocan could, in turn, modulate some of the subsequent events involving the vasculature. Vascularization of the RPE by retinal vessels occurs, for instance, in RCS rats in areas where photoreceptors and outer segment debris have disappeared. As shown previously[64] and in the present study, RPE cells are present along retinal vessels and in the vitreous margin of the retina in RCS rat retinas. RPE-associated changes in the composition and thickness of the perivascular matrix have been suggested to modulate, at least in part, the migration and proliferation of retinal endothelial cells.[58] An accumulation of neurocan was present around the vessels long before RPE cells were visible intraretinally. This indicates that migrated RPE cells are not, at least at the initial stages, the primary source of the accumulated neurocan. It is possible, however, that the neurocan accumulated perivascularly ultimately creates, through interactions with other matrix molecules, a substrate for the migration of the RPE cells. Versican, another hyaluronan-binding matrix proteoglycan, and decorin, which, along with versican, has been detected in the normal retina,[12,65] have been suggested to play a role in proliferative diabetic retinopathy and in the formation of epiretinal membranes in proliferative vitreoretinopathy.[66,67]

In contrast to the situation observed in normal retinas, neurocan was clearly detected by immunoblot analysis in adult RCS rats. The predominant 150-kDa band conformed with the proteolytic state normally observed in brain at this age.[23] It could also point to a glial origin, given that an increased astrocytic expression of neurocan occurs after neuronal injury,[29,30] and that cleavage of neurocan can occur intracellularly in astrocytes,[31] possibly by the protease MMP-2, which has been found to be expressed in these cells.[55] Accumulation of neurocan was not observed in the Müller cells themselves in RCS rats; however, the possibility might be considered that these cells are somehow involved in the process of accumulation or are even a source of the accumulated neurocan.

It is not possible, however, to establish at this point what exactly triggers the accumulation of neurocan around vessels in RCS rats, which cell(s) may be involved, whether neurocan plays a role in the vasculature, or which role it plays. No neurocan labeling was detected in our study in association with normal retinal vascular development. Further, although some accumulation of neurocan was associated with vessels in P23H and S334ter rats, it was far less prominent than in RCS rats, and occurred long after photoreceptor cells started to die. Not much is yet known about vascular changes that occur in the mutant rhodopsin transgenic rats that we studied. However, vascular changes have been reported in several other animal models of photoreceptor cell degeneration and in human retinitis pigmentosa, and alterations of the perivascular matrix have also been observed in many of these cases.[19,41,42,63,68]

The observations in the present study thus indicate that vessel-associated accumulation of neurocan can occur, but is not a general phenomenon or even a common feature of all types of photoreceptor cell degeneration. It appears instead that the particular conditions created in the subretinal space in RCS rats are what trigger the abnormal accumulation. Mutations in *MERTK*, the human orthologue of the RCS rat retinal dystrophy gene, have also been identified in patients with degenerative retinal disease,[69] and it is conceivable that similar vascular alterations occur in the retinas of these individuals. Neurocan and another CS-PG, phosphacan, have been shown to bind with high affinity to fibroblast growth factor (FGF)-2,[70] an angiogenic factor.[71] Increased levels of FGF-2 are noted in RCS rats.[72] There is thus the possibility that binding of accumulated neurocan to this or other growth factors is directly or indirectly involved in some of the vascular changes observed in RCS rats and perhaps also in patients with *MERTK* mutations.

Acknowledgments

The authors thank Berndt Ehinger and Reinhard Fässler (Lund University) for support, Olaf Strauss (Freie University, Berlin, Germany) for providing the RCS-*rdy*$^+$ rats with nondystrophic retinas, and Karin Arnér and Gunnel Roos for technical assistance.

References

1. Iozzo RV. Matrix proteoglycans: from molecular design to cellular function. *Annu Rev Biochem.* 1998;67:609–652.
2. Lander AD. Proteoglycans in the nervous system. *Curr Opin Neurobiol.* 1993;3:716–723.
3. Aquino DA, Margolis RU, Margolis RK. Immunocytochemical localization of a chondroitin sulfate proteoglycan in nervous tissue. I. Adult brain, retina, and peripheral nerve. *J Cell Biol.* 1984;99:1117–1129.
4. Porrello K, LaVail MM. Histochemical demonstration of spatial heterogeneity in the interphotoreceptor matrix of the rat retina. *Invest Ophthalmol Vis Sci.* 1986;27:1577–1586.
5. Hageman GS, Johnson LV. Chondroitin 6-sulfate glycosaminoglycan is a major constituent of primate cone photoreceptor matrix sheaths. *Curr Eye Res.* 1987;6:639–646.
6. Stramm LE. Synthesis and secretion of glycosaminoglycans in cultured retinal pigment epithelium. *Invest Ophthalmol Vis Sci.* 1987;28:618–627.
7. Threlkeld A, Adler R, Hewitt AT. Proteoglycan biosynthesis by chick embryo retina glial-like cells. *Dev Biol.* 1989;132:559–568.
8. Landers RA, Tawara A, Varner HH, Hollyfield JG. Proteoglycans in the mouse interphotoreceptor matrix. IV. Retinal synthesis of chondroitin sulfate proteoglycan. *Exp Eye Res.* 1991;52:65–74.
9. Murillo-Lopez F, Politi L, Adler R, Hewitt AT. Proteoglycan synthesis in cultures of murine retinal neurons and photoreceptors. *Cell Mol Neurobiol.* 1991;11:579–591.
10. Brittis PA, Canning DR, Silver J. Chondroitin sulfate as a regulator of neuronal patterning in the retina. *Science.* 1992;255:733–736.

11. Williams C, Villegas M, Atkinson R, Miller CA. Chondroitin sulfate proteoglycan specific to retinal horizontal neurons. *J Comp Neurol.* 1998;390:268–277.
12. Inatani M, Tanihara H, Honjo M, Hangai M, Kresse H, Honda Y. Expression of proteoglycan decorin in neural retina. *Invest Ophthalmol Vis Sci.* 1999;40:1783–1791.
13. Inatani M, Tanihara H, Oohira A, Honjo M, Honda Y. Identification of a nervous tissue-specific chondroitin sulfate proteoglycan, neurocan, in developing rat retina. *Invest Ophthalmol Vis Sci.* 1999; 40:2350–2359.
14. Inatani M, Tanihara H, Oohira A, et al. Neuroglycan C, a neural tissue-specific transmembrane chondroitin sulfate proteoglycan, in retinal neural network formation. *Invest Ophthalmol Vis Sci.* 2000;41:4338–4346.
15. LaVail MM, Pinto LH, Yasumura D. The interphotoreceptor matrix in rats with inherited retinal dystrophy. *Invest Ophthalmol Vis Sci.* 1981;21:658–668.
16. Schmidt SY, Heth CA, Edwards RB, et al. Identification of proteins in retinas and IPM from eyes with retinitis pigmentosa. *Invest Ophthalmol Vis Sci.* 1988;29:1585–1593.
17. Tawara A, Hollyfield JG. Proteoglycans in the mouse interphotoreceptor matrix. III. Changes during photoreceptor development and degeneration in the *rds* mutant. *Exp Eye Res.* 1990;51:301–315.
18. LaVail MM, White MP, Gorrin GM, Yasumura D, Porrello KV, Mullen RJ. Retinal degeneration in the nervous mutant mouse. I. Light microscopic cytopathology and changes in the interphotoreceptor matrix. *J Comp Neurol.* 1993;333:168–181.
19. Blanks JC, Johnson LV. Vascular atrophy in the retinal degenerative *rd* mouse. *J Comp Neurol.* 1986;254:543–553.
20. Farber DB, Flannery JG, Bowes-Rickman C. The *rd* mouse story: seventy years of research on an animal model of inherited retinal degeneration. *Prog Retinal Eye Res.* 1994;13:31–64.
21. Villegas-Perez MP, Vidal-Sanz M, Lund RD. Mechanism of retinal ganglion cell loss in inherited retinal dystrophy. *Neuroreport.* 1996;7:1995–1999.
22. Milam AH, Li ZY, Fariss RN. Histopathology of the human retina in retinitis pigmentosa. *Prog Retinal Eye Res.* 1998;17:175–205.
23. Rauch U, Gao P, Janetzko A, et al. Isolation and characterization of developmentally regulated chondroitin sulfate and chondroitin/keratan sulfate proteoglycans of brain identified with monoclonal antibodies. *J Biol Chem.* 1991;266:14785–14801.
24. Margolis RK, Rauch U, Maurel P, Margolis RU. Neurocan and phosphacan: two major nervous tissue-specific chondroitin sulfate proteoglycans. *Perspect Dev Neurobiol.* 1996;3:273–290.
25. Oohira A, Matsui F, Tokita Y, Yamauchi S, Aono S. Molecular interactions of neural chondroitin sulfate proteoglycans in the brain development. *Arch Biochem Biophys.* 2000;374:24–34.
26. Meyer-Puttlitz B, Junker E, Margolis RU, Margolis RK. Chondroitin sulfate proteoglycans in the developing central nervous system. II. Immunocytochemical localization of neurocan and phosphacan. *J Comp Neurol.* 1996;366:44–54.
27. Milev P, Maurel P, Haring M, Margolis RK, Margolis RU. TAG-1/axonin-1 is a high-affinity ligand of neurocan, phosphacan/protein-tyrosine phosphatase-zeta/beta, and N-CAM. *J Biol Chem.* 1996; 271:15716–15723.
28. Inatani M, Tanihara H, Oohira A, Honjo M, Kido N, Honda Y. Upregulated expression of neurocan, a nervous tissue specific proteoglycan, in transient retinal ischemia. *Invest Ophthalmol Vis Sci.* 2000;41:2748–2754.
29. Haas CA, Rauch U, Thon N, Merten T, Deller T. Entorhinal cortex lesion in adult rats induces the expression of the neuronal chondroitin sulfate proteoglycan neurocan in reactive astrocytes. *J Neurosci.* 1999;19:9953–9963.
30. McKeon RJ, Jurynec MJ, Buck CR. The chondroitin sulfate proteoglycans neurocan and phosphacan are expressed by reactive astrocytes in the chronic CNS glial scar. *J Neurosci.* 1999;19:10778–10788.
31. Asher RA, Morgenstern DA, Fidler PS, et al. Neurocan is upregulated in injured brain and in cytokine-treated astrocytes. *J Neurosci.* 2000;20:2427–2438.
32. D'Cruz PM, Yasumura D, Weir J, et al. Mutation of the receptor tyrosine kinase gene mertk in the retinal dystrophic RCS rat. *Hum Mol Genet.* 2000;9:645–651.
33. Dowling JE, Sidman RL. Inherited retinal dystrophy in the rat. *J Cell Biol.* 1962;14:73–109.
34. Mullen RJ, LaVail MM. Inherited retinal dystrophy: primary defect in pigment epithelium determined with experimental rat chimeras. *Science.* 1976;192:799–801.
35. Eisenfeld AJ, Bunt-Milam AH, Sarthy PV. Müller cell expression of glial fibrillary acidic protein after genetic and experimental photoreceptor degeneration in the rat retina. *Invest Ophthalmol Vis Sci.* 1984;25:1321–1328.
36. Caldwell RB, Roque RS, Solomon SW. Increased vascular density and vitreo-retinal membranes accompany vascularization of the pigment epithelium in the dystrophic rat retina. *Curr Eye Res.* 1989;8:923–937.
37. Härtig W, Grosche J, Distler C, Grimm D, el-Hifnawi E, Reichenbach A. Alterations of Muller (glial) cells in dystrophic retinae of RCS rats. *J Neurocytol.* 1995;24:507–517.
38. Villegas-Perez MP, Lawrence JM, Vidal-Sanz M, Lavail MM, Lund RD. Ganglion cell loss in RCS rat retina: a result of compression of axons by contracting intraretinal vessels linked to the pigment epithelium. *J Comp Neurol.* 1998;392:58–77.
39. Liu C, Li Y, Peng M, Laties AM, Wen R. Activation of caspase-3 in the retina of transgenic rats with the rhodopsin mutation S334ter during photoreceptor degeneration. *J Neurosci.* 1999;19:4778–4785.
40. Machida S, Kondo M, Jamison JA, et al. P23H rhodopsin transgenic rat: correlation of retinal function with histopathology. *Invest Ophthalmol Vis Sci.* 2000;41:3200–3209.
41. Matthes MT, Bok D. Blood vascular abnormalities in the degenerative mouse retina (C57BL/6J-rd le). *Invest Ophthalmol Vis Sci.* 1984;25:364–369.
42. Nishikawa S, LaVail MM. Neovascularization of the RPE: temporal differences in mice with rod photoreceptor gene defects. *Exp Eye Res.* 1998;67:509–515.
43. Wang S, Villegas-Perez MP, Vidal-Sanz M, Lund RD. Progressive optic axon dystrophy and vascular changes in rd mice. *Invest Ophthalmol Vis Sci.* 2000;41:537–545.
44. Thon N, Haas CA, Rauch U, et al. The chondroitin sulphate proteoglycan brevican is upregulated by astrocytes after entorhinal cortex lesions in adult rats. *Eur J Neurosci.* 2000;12:2547–2558.
45. Zhou XH, Brakebusch C, Matthies H, et al. Neurocan is dispensable for brain development. *Mol Cell Biol.* 2001;21:5970–5978.
46. Li H, Leung TC, Hoffman S, Balsamo J, Lilien J. Coordinate regulation of cadherin and integrin function by the chondroitin sulfate proteoglycan neurocan. *J Cell Biol.* 2000;149:1275–1288.
47. Inatani M, Honjo M, Otori Y, et al. Inhibitory effects of neurocan and phosphacan on neurite outgrowth from retinal ganglion cells in culture. *Invest Ophthalmol Vis Sci.* 2001;42:1930–1938.
48. Acharya S, Rayborn ME, Hollyfield JG. Characterization of SPACR, a sialoprotein associated with cones and rods present in the interphotoreceptor matrix of the human retina: immunological and lectin binding analysis. *Glycobiology.* 1998;8:997–1006.
49. Hollyfield JG. Hyaluronan and the functional organization of the interphotoreceptor matrix. *Invest Ophthalmol Vis Sci.* 1999;40: 2767–2769.
50. Hollyfield JG, Rayborn ME, Midura RJ, Shadrach KG, Acharya S. Chondroitin sulfate proteoglycan core proteins in the interphotoreceptor matrix: a comparative study using biochemical and immunohistochemical analysis. *Exp Eye Res.* 1999;69:311–322.
51. Acharya S, Foletta VC, Lee JW, et al. SPACRCAN, a novel human interphotoreceptor matrix hyaluronan-binding proteoglycan synthesized by photoreceptors and pinealocytes. *J Biol Chem.* 2000; 275:6945–6955.
52. Turk BE, Huang LL, Piro ET, Cantley LC. Determination of protease cleavage site motifs using mixture-based oriented peptide libraries. *Nat Biotechnol.* 2001;19:661–667.
53. Padgett LC, Lui GM, Werb Z, LaVail MM. Matrix metalloproteinase-2 and tissue inhibitor of metalloproteinase-1 in the retinal pigment epithelium and interphotoreceptor matrix: vectorial secretion and regulation. *Exp Eye Res.* 1997;64:927–938.

54. Weidman TA, Kuwabara T. Postnatal development of the rat retina: an electron microscopic study. *Arch Ophthalmol.* 1968;79: 470–484.
55. Agapova OA, Ricard CS, Salvador-Silva M, Hernandez MR. Expression of matrix metalloproteinases and tissue inhibitors of metalloproteinases in human optic nerve head astrocytes. *Glia.* 2001;33: 205–216.
56. Eisenfeld AJ, Bunt-Milam AH, Saari JC. Immunocytochemical localization of interphotoreceptor retinoid-binding protein in developing normal and RCS rat retinas. *Invest Ophthalmol Vis Sci.* 1985; 26:775–778.
57. Chaitin MH, Brun-Zinkernagel AM. Immunolocalization of CD44 in the dystrophic rat retina. *Exp Eye Res.* 1998;67:283–292.
58. Caldwell RB, Slapnick SM, Roque RS RP. E-associated extracellular matrix changes accompany retinal vascular proliferation and retino-vitreal membranes in a new model for proliferative retinopathy: the dystrophic rat. *Prog Clin Biol Res.* 1989;314:393–407.
59. Weber ML, Mancini MA, Frank RN. Retinovitreal neovascularization in the Royal College of Surgeons rat. *Curr Eye Res.* 1989;8: 61–74.
60. LaVail MM, Sidman RL, O'Neil D. Photoreceptor-pigment epithelial cell relationships in rats with inherited retinal degeneration: radioautographic and electron microscope evidence for a dual source of extra lamellar material. *J Cell Biol.* 1972;53:185–209.
61. Chu Y, Walker LN, Vijayasekaran SL, Cooper RL, Porrello KV, Constable IJ. Developmental study of chondroitin-6-sulphate in normal and dystrophic rat retina. *Graefes Arch Clin Exp Ophthalmol.* 1992;230:476–482.
62. Roque RS, Caldwell RB. Müller cell changes precede vascularization of the pigment epithelium in the dystrophic rat retina. *Glia.* 1990;3:464–475.
63. Fariss RN, Apte SS, Luthert PJ, Bird AC, Milam AH. Accumulation of tissue inhibitor of metalloproteinases-3 in human eyes with Sorsby's fundus dystrophy or retinitis pigmentosa. *Br J Ophthalmol.* 1998;82:1329–1334.
64. Roque RS, Caldwell RB. Pigment epithelial cell changes precede vascular transformations in the dystrophic rat retina. *Exp Eye Res.* 1991;53:787–798.
65. Zako M, Shinomura T, Ujita M, Ito K, Kimata K. Expression of PG-M(V3), an alternatively spliced form of PG-M without a chondroitin sulfate attachment in region in mouse and human tissues. *J Biol Chem.* 1995;270:3914–3918.
66. Hagedorn M, Esser P, Wiedemann P, Heimann K. Tenascin and decorin in epiretinal membranes of proliferative vitreoretinopathy and proliferative diabetic retinopathy. *Ger J Ophthalmol.* 1993;2: 28–31.
67. Imagawa M, Zako M, Mizutani S, et al. Increased expression of versican in tissues from proliferative diabetic retinopathy patients [ARVO Abstract]. *Invest Ophthalmol Vis Sci.* 2000;41(4):**S**652. Abstract nr 3464.
68. Penn JS, Li S, Naash MI. Ambient hypoxia reverses retinal vascular attenuation in a transgenic mouse model of autosomal dominant retinitis pigmentosa. *Invest Ophthalmol Vis Sci.* 2000;41:4007–4013.
69. Gal A, Li Y, Thompson DA, et al. Mutations in MERTK, the human orthologue of the RCS rat retinal dystrophy gene, cause retinitis pigmentosa. *Nat Genet.* 2000;26:270–271.
70. Milev P, Monnerie H, Popp S, Margolis RK, Margolis RU. The core protein of the chondroitin sulfate proteoglycan phosphacan is a high-affinity ligand of fibroblast growth factor-2 and potentiates its mitogenic activity. *J Biol Chem.* 1998;273:21439–21442.
71. Cross MJ, Claesson-Welsh L. FGF and VEGF function in angiogenesis: signalling pathways, biological responses and therapeutic inhibition. *Trends Pharmacol Sci.* 2001;22:201–207.
72. Bugra K, Hicks D. Acidic and basic fibroblast growth factor messenger RNA and protein show increased expression in adult compared to developing normal and dystrophic rat retina. *J Mol Neurosci.* 1997;9:13–25.